Chapter 5

Double Resonance

5.1 Introduction

Many experiments on two and three level atoms using multiple fields, aim at studying the interaction between radiation and matter. Such experiments measure the absorption of a weak probe that has counter-propagating to it a strong beam of the same frequency. This enables the selection, from a hot gas, of atoms with zero velocity along the direction of the two beams. It is in this configuration that one studies narrow spectral features, that could otherwise not have been resolved due to the Doppler broadening. This very idea is used even in saturated absorption spectroscopy, where hyperfine transitions of a few MHz width may be resolved.

By the same argument, measurements of the fluorescence from the atoms are not expected to display narrow spectral features as they are emissions from a collection of randomly moving atoms, and will be Doppler broadened. We describe below our experiments on ^{85}Rb atoms, where dips in the fluorescence as narrow as 6 MHz, and peaks with widths of about 30MHz ($\ll$ Doppler width $\sim$ 2 GHz at the room temperature) have been quite easily observed. These are seen when two distinct transitions are addressed by two laser fields. We explain this as a consequence of narrow velocity selection due to double-resonance, and propose that this technique may be used to select out a particular velocity class of atoms (with non-zero velocity component along the direction of the photon) from thermal ensemble of hot atoms.

5.2 Experiment

In our experiment we use two external cavity diode lasers, locked to the $F = 3 -> F' = 4$ and $F = 2 -> F' = 3$ (or 2) transitions for the cooling and the repumper beams respectively. The beams from each of the two lasers were split into four parts, one of which was sent to a Doppler-free saturated absorption setup in a vapour cell that was used to determine the instantaneous frequency of the laser when it was ramped or was used for locking the frequency. The remaining three beams from each laser were incident into the chamber from the +X, +Y and +Z directions, and were retroreflected, to form three pairs of counter-propagating, mutually orthogonal beams, that intersected at the centre of the chamber. This forms an optical molasses when the cooling beam is detuned to within a few linewidths to the red of the $F = 3$ to $F' = 4$ transition.

Schematic of this experimental setup is shown in figure 5.1, and a photograph is shown in figure 5.2. This photo differs from the photo of the MOT shown in chapter 2, in that the magnetic coils are removed. The atoms are cooled and slowed down in the optical molasses but are not trapped. The diameter of the beams was about 1 cm, and thus the molasses region was a cube of side 1 cm. Each cooling beam was of intensity 2 mW/cm^2, and the repumper 0.1 mW/cm^2(one order less intense). A femtowatt detector (New Focus, Model 2151) was placed at one of the viewports and a camera zoom lens system imaged the fluorescent light from the centre of the chamber onto the detector. Most of the data presented in this chapter is this fluorescence. However in addition, we performed absorption experiments using a probe beam(figure 5.1). This probe beam passes through the chamber and gets reflected back normally at a mirror, so as to overlap with the forward beam. The intensity of the reflected beam, however, is weaker because of its passage twice through the glass window. Because of this, the resulting configuration of the two beams is like the Doppler-free pump-probe configuration. This reflected beam is made incident on a photo detector so as to measure its absorption. The results of the fluorescence studies are discussed first. Towards the end of the

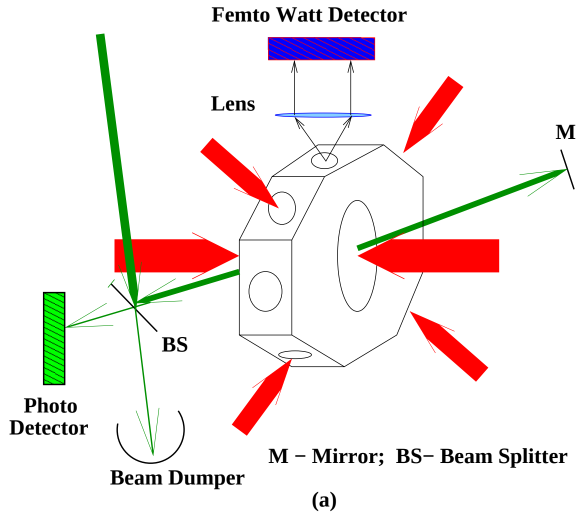

Figure 5.1: Schematic experimental setup: showing the octagonal vaccum chamber. The thick red lines are the cooling and repumper beams. The green line is the probe beam. Probe beam is retro-reflected so that the absorption is studied in the Doppler free configuration.

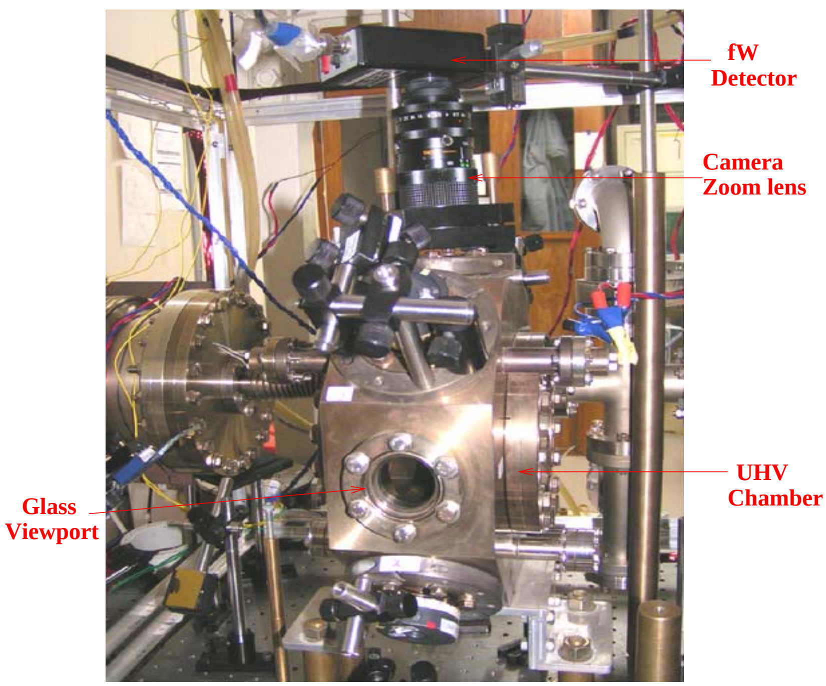

Figure 5.2: The experimental setup. We have used the same MOT chamber but magnetic coils were removed.

chapter the absorption results are given.

Fluorescence from the atoms was studied when they were driven by the two fields, the cooling and the repumper laser fields. The cooling laser was locked at various detunings δ_c in the range +120 MHz (blue) to -200 MHz (red) with respect to the cooling transition. The detunings thus spanned a region much greater than the width($\sim$ 180 MHz) of the full hyperfine manifold F = 3 $->$ F$'$. At each detuning the repumper laser was scanned very slowly (with a period of 20 s) across its hyperfine manifold F = 2 $->$ F$'$. To study the fluorescence signal we record the femtowatt detector output in one of the channels of the oscilloscope while the saturated absorption signal of the repumper was recorded in the other channel. The latter gave the instantaneous repumper frequency.

It may be mentioned here that cooling of the atoms occur when the cooling laser is detuned to the red within a few linewidths of the cooling transition(natural linewidth $\Gamma =\sim 6$ MHz). In our experiment, however, the detunings are often quite large, and in many cases to the blue of the cooling transition. Even though the “cooling” beam does not cool, nor does the “molasses” provide a retarding force, we retain terms like “cooling” and “molasses”.

5.3 The experimental results

The dependence of the fluorescence signal on the detunings of the two driving fields is shown in figure 5.3 for $\delta_c < 0$ and figure 5.4 for $\delta_c > 0$. In both figures, upper-most trace shows the saturated absorption spectrum of the repumper as it is scanned across $F = 2- > F'$, providing a measure of the instantaneous repumper frequency. The remaining traces display the instantaneous fluorescence intensity collected from the molasses region, for various detunings of the cooling laser, arising from the F = 3 $- > F' = 4$ cooling transition. Trace A in both figures shows the fluorescence from the molasses with the cooling laser on resonance. The fluorescence shows two maxima, (labelled ‘a’ and ‘b’), corresponding to the two repumping transitions. For small detunings of the cooling laser (trace B in both figures 5.3 and 5.4), narrow dips appear in the fluorescence signal, splitting the peaks a and b. These are centred at the points where the repumper laser is exactly resonant to the repumping transitions. Each of the peaks a and b splits into a pair of peaks, labelled a_+, a_- and b_+, b_-, symmterically displaced from the original peaks, a and b. As the cooling laser is progressively detuned, each pair a_+, a_- and b_+ , b_- separate further (Traces C-E in 5.3 and 5.4) resulting in four distinct peaks in the fluorescence signal. The width of each peak remains fairly constant at 30 MHz. In several cases, there appear some very weak peaks,

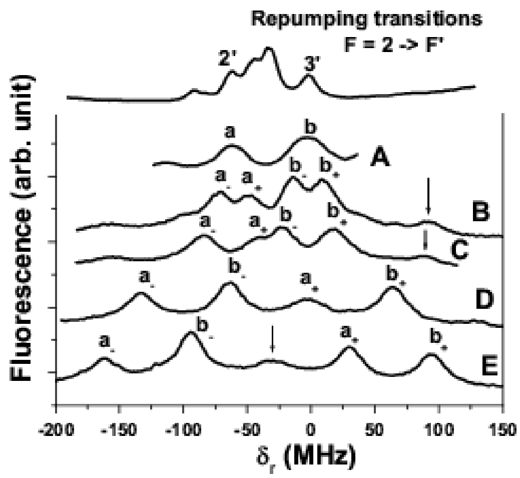

Figure 5.3: Fluorescence signal from the molasses for red detuning of the cooling laser as a function of the instantaneous repumper frequency. The upper-most trace gives the saturation absorption spectrum of the repumper laser. Traces A-E correspond to $\delta_c = 0, -12, -22, -60$ and -92 MHz respectively.

indicated by arrows. These peaks are well resolved only for large detunings of the cooling laser. In figure 5.5, the frequency shift of each of the four peaks with respect to the repumper transition ($F = 2- > F' = 3$) is plotted as a function of the detuning of the cooling laser δ_c. The peak positions fall on straight lines with slopes ±1; the two lines corresponding to the + and - peaks of each transition intersect when the detuning of the cooling laser is zero. The intercepts are separated by ~ 63 MHz.

It can be deduced from the following that the fluorescence is from the cooling transition. When only the repumper beam is allowed into the chamber the fluorescence is weak (~ 2 mV)(figure 5.6(A)), as opposed to a stronger fluorescence (~ 50 mV) when the cooling

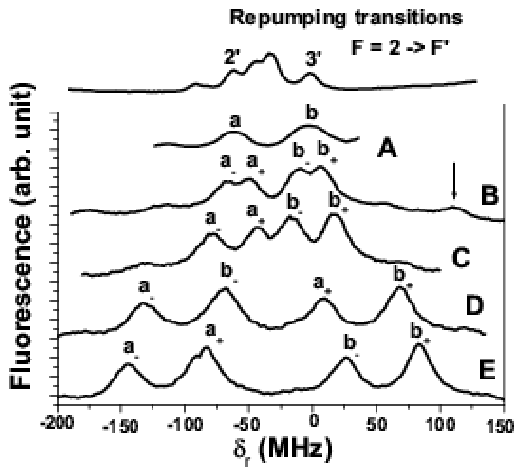

Figure 5.4: Fluorescence signal from the molasses for blue detuning of the cooling laser as a function of the instantaneous repumper frequency. The upper-most trace gives the saturation absorption spectrum of the repumper laser. Traces A-E correspond to $0, 10, 20, 70$ and 90 MHz respectively

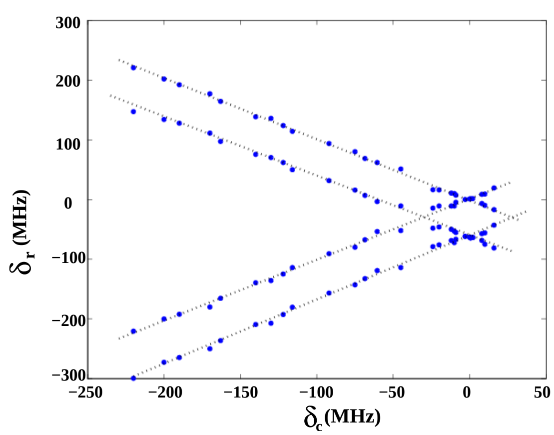

Figure 5.5: The positions of the fluorescence peaks as a function of the detuning of the cooling laser. The dotted lines have slopes ±1 and are drawn by hand. $\delta_r = 0$ corresponds to the $2- > 3'$ transition.

beam is also incident on the atoms (figure 5.6(B)). All the results presented here, have fluorescence in the 50 mV range, indicating that it is predominantly from the cooling transition. We note that while $F = 2 -> F' = 1, 2, 3$ are allowed transitions, because of the selection rule of the transition, only $F = 2 -> F' = 2, 3$ serve to repump atoms back into the cooling cycle. As we see enhanced fluorescence only when the repumper laser is close to either of these transitions (figure 5.6(B)), it confirms that it is predominantly the cooling transition that contributes to the fluorescence.

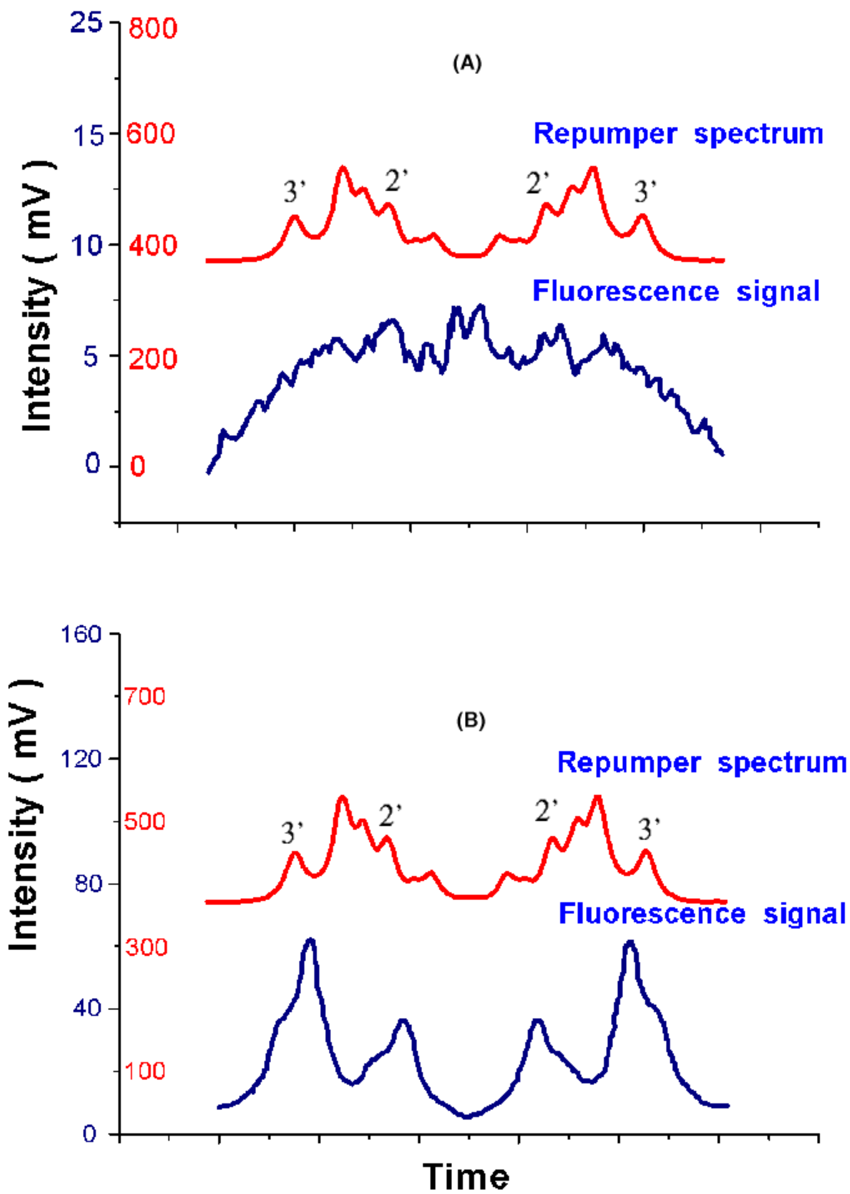

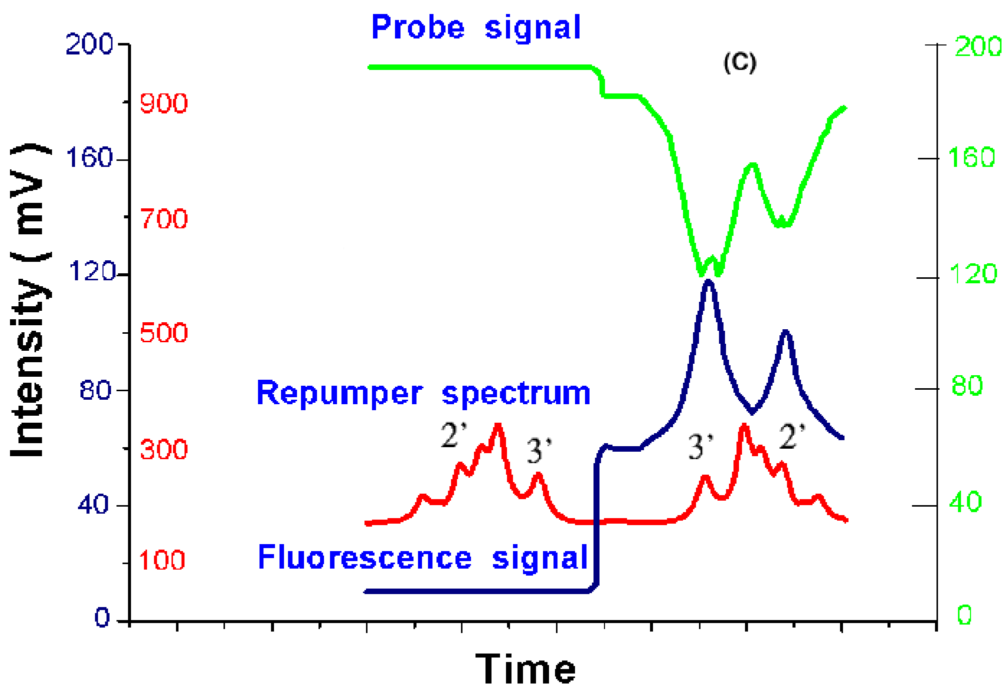

Figure 5.6: Experiment to verify that the fluorescence is predominantly from the cooling transition. In all three cases the red colour trace is the saturated absorption signal of the frequency scanned repumper and is a measure of the instantaneous repumper frequency. The other traces are as follows: Blue trace in (A) is the fluorescence from the molasses region when only the repumper is incident. Blue trace in (B) is the fluorescence from the molasses region when both repumper and cooling beams are present. In (C) the blue trace is the fluorescence and the green trace is the probe (cooling laser) absorption in the molasses. The scales for the different signals are drawn with the colour same as the corresponding trace.

Figure 5.6(C) illustrates an interesting feature. This figure has three traces the saturated absorption spectrum of the repumper laser (red) which is periodically scanned across $F = 2 -> F'$ manifold, the fluorescence signal from the molasses (blue) and the absorption of a weak probe (green) derived from the cooling laser which is locked to the $F = 3 -> F' = 4$ transition. For the first half of the traces, the repumper laser to the molasses is blocked. During this period, the fluorescence and the absorption signals are unchanged in time, which is as they should be, as the cooling laser is locked. In the later half, the cooling laser continued to be locked, but the repumper, with its frequency being periodically scanned, was allowed into the molasses region. Therefore, the presence of the repumper dramatically alters the absorption of the cooling laser, as is seen from the probe signal (green). Further, as the fluorescence signal (blue) is roughly similar (though inverted) to the probe absorption signal, it is reasonable to conclude that the light absorbed from the cooling beam by the atom is spontaneously emitted in random directions, and forms the fluorescence signal.

It may be noted that in our experiment we are not performing any frequency analysis of the emitted fluorescent light, but we are studying the fluorescence response of the atoms to the repumper laser that is being frequency scanned. The various spectral features occur at the same relative positions to the repumper peaks for all slow rates of scan of the repumper frequency.

5.3.1 Autler Townes Doublet

We tried to understand the cause for the splitting of peaks. The narrow spectral features seemed to suggest a quantum phenomenon. We first examined this possibility. In our experiment cooling(pump) laser can drive the atoms coherently between the ground and excited states. This driving creates the “dressed ” states whose energies are shifted depending on the strength of the drive. This is also called the ac Stark shift[1]. In the presence of the dressed states, the probe-absorption spectrum should split into two peaks, called an Autler Townes doublet[2]. The location of the two peaks is given by [3, 4].

$$\Delta_{\pm} = (1/2)[\Delta_p \pm (\Delta_p^2 + \Omega^2)^{1/2}] \tag{5.1}$$

where, Δ_p and Ω are the detuning and the intensity of the pump laser respectively. Δ_+ and Δ_- are the values of the probe detuning where the peaks occur. The corresponding linewidths

($\Gamma_\pm$) of these peaks are also different, and given by

$$\Gamma_\pm = \frac{\Gamma}{2}\left(1 \mp \frac{\Delta_p}{\sqrt{\Delta_p^2 + \Omega^2}}\right) \tag{5.2}$$

It is clear from the above expression that, if $\Delta_p = 0$, the two peaks are symmetric and have identical linewidths of $\Gamma/2$. However, for any non-zero detuning the peaks have asymmetric linewidths. The first peak has larger linewidth, while the second peak has smaller linewidth by precisely the same factor, in such a way that the sum of the two linewidths is equal to the unperturbed linewidth, Γ.

The above analysis is valid for a stationary atom. If the atom is moving, the laser detuning as seen by the atom depends on its velocity. To obtain the probe absorption in a gas of moving atoms, the above expressions have to be corrected for the velocity of the atom and then averaged over the Maxwell-Boltzmann distribution of velocities. Such an analysis has been done by Vemuri et al. in reference[4]. The important conclusion of that work is that the location of the peaks given in equation 5.1 does not change, but the line-widths are now given by

$$\Gamma_\pm = \frac{(\Gamma + D)}{2}\left(1 \mp \frac{\Delta_p}{\sqrt{\Delta_p^2 + \Omega^2}}\right). \tag{5.3}$$

Here, D is the Doppler width.

In our experiment, we do indeed see maximal repumping efficiency for two values of the repumper frequency about each repumping transition (figures 5.3 and 5.4 trace B). However, the peaks are equal in width and they are symmetrically displaced about their unsplit position which is unlike the Autler-Townes doublet, where for example, for small Ω, the shifts are 0 and Δ_p. So a different mechanism seems to be operative.

5.3.2 The Double Resonance Model

To understand the experimental results we propose a model for the absorption of the photons by the atoms. We know that the maximum fluorescence from the atoms is obtained when atoms are repumped from F = 2 level to F = 3 level, and then raised to $F' = 4$. This requires the enhanced transition rates from F = 2 − > F' = 3 and F = 3 − > F' = 4 or, F = 2 − > F' = 2 and F = 3 − > F' = 4, or equivalently, increased absorption rates of a repumper photon and a cooling photon. The requirement that the two photons be absorbed, in turn, requires that the detuning of the two lasers be compensated for by the Doppler shift. Therefore this model provides a means of velocity selection where atoms of a particular velocity can be selected depending on the detuning of the cooling (pump) laser. This is in contrast to the conventional Doppler-free saturated absorption, where only zero-velocity atoms are selected out as described earlier.

For an atom with velocity **v**, and cooling beam of detuning δ_c, absorption is maximised when $\mathbf{k} \cdot \mathbf{v} = -\delta_{\mathbf{c}}$. The repumper, which serves to bring atoms back to the cooling cycle, will be most effective for this velocity class of atoms only when its detuning $\delta_r = \pm \mathbf{k} \cdot \mathbf{v}$. The '+' (-) sign is for the repumper beam counter- (co-) propagating to the cooling beam. Both possibilities exist in our experiment. If $\delta_r \neq \pm \mathbf{k} \cdot \mathbf{v}$ repumping will not occur and the fluorescence from the cooling transition will be diminished. This is precisely what is seen in the experiment. The slopes ± 1 in figure 5.5 indicate that the maximum fluorescence occurs only when $\delta_c = \pm \delta_r$, that is, only when the resonance condition is simultaneously satisfied for both the cooling and repumper beams. Since we have two repumper transitions we see two pairs of lines. For $\delta_c = 0$ the two pairs of lines converge at $\delta_r \approx 0$ and $\delta_r \approx -63$ MHz, this being the hyperfine interval between $F' = 3$ and $F' = 2$ (figure 5.5). This suggests a means of determining hyperfine intervals to good accuracy.

To verify the validity of this model, experiments were performed for various configurations of co- and counter- propagation of the laser beams. The results are shown in figure 5.7. When the cooling and repumper beams both are in the same direction (**k**), an atom with velocity **v**, sees their frequencies as $\omega_c + \delta_c - \mathbf{k} \cdot \mathbf{v}$ and $\omega_r + \delta_r - \mathbf{k} \cdot \mathbf{v}$. For the two transitions to be simultaneously on resonance, we require $\delta_c = \delta_r = \mathbf{k} \cdot \mathbf{v}$. The experiment did indeed yield a peak at $\delta_r = \delta_c$ only. For the case, where the repumper is counter-propagating to the cooling beam, an atom of velocity v will see the laser frequencies at $\omega_r + \delta_r + \mathbf{k} \cdot \mathbf{v}$ and $\omega_c + \delta_c - \mathbf{k} \cdot \mathbf{v}$, giving the condition $\delta_c = -\delta_r$ for simultaneous resonance of the two transitions, and once again the experiment proves this. When the cooling and repumper beams are incident in both directions, peaks appear at both $\pm\delta_c$, confirming that simultaneous Doppler resonance is the origin of the symmetric pairs of fluorescence peaks. This, surprisingly, gives rise to a fluorescence spectrum of line width as narrow as 30 MHz from a collection of atoms of Doppler width $\approx$ 2 GHz.

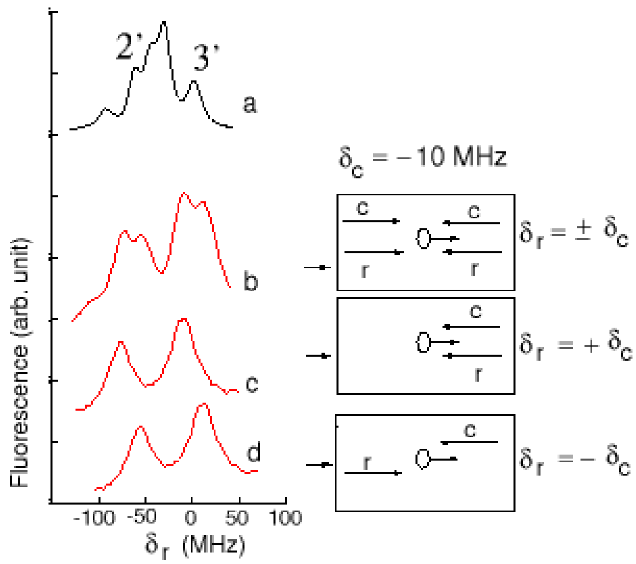

Figure 5.7: Experimental verification of the Double Resonance Model. Trace a: Saturation absorption signal of the repumper. Trace b, c and d are the fluorescence signals obtained for the beam configurations shown alongside.

5.4 Analytic calculation of fluorescence peaks

We now give an analytical derivation of the fluorescence spectra to show that the narrow fluorescent peaks will indeed arise upon double resonance. For simplicity, we consider beams along the $\pm$ z direction only. When the atoms enter the molasses region, one half of the atoms of any velocity v are in the $F = 2$ level and the other half in the $F = 3$ level. In our calculation we consider the repumping transition through $F' = 3$ only. If the laser fields are switched on the redistribution of the atoms between the two ground states take place. The rate at which the cooling beam transfers atoms from $F = 3$ to the upper level $F' = 3$ is given by (see eqn.3.14, [5])

$$\eta_{33'} = \Gamma_{3'3} \frac{\frac{I_c}{I_{s33'}}}{[1 + 2(I_c/I_{s33'}) + 4(\Delta_{3'3}/\Gamma_{3'3})^2]} \tag{5.4}$$

where, I_c = Intensity of the cooling beam, Γ_{ij} = linewidth of the transitions between states i and j, I_{sij} = saturation intensity of the transition from i to j, $\Delta_{3'3} = \Delta_c + 121$ MHz , $\Delta_c = \delta_c$ -$\mathbf{k} \cdot \mathbf{v}$. From the level $F' = 3$ the atoms can come down to both $F = 2$ and $F = 3$ level. Therefore, the rate at which the cooling beam transfers atoms from $F = 3$ to $F = 2$ through the upper level $F' = 3$ is given by

$$\begin{aligned} \eta_{32} &= \eta_{33'} \frac{\Gamma_{3'2}}{(\Gamma_{3'3} + \Gamma_{3'2})} \\ &= \Gamma_{3'3} \frac{\frac{I_c}{I_{s33'}}}{[1 + 2(I_c/I_{s33'}) + 4(\Delta_{3'3}/\Gamma_{3'3})^2]} \frac{\Gamma_{3'2}}{(\Gamma_{3'3} + \Gamma_{3'2})} \end{aligned} \tag{5.5}$$

Here the product of the first two factors indicates the rate at which atoms are transferred to the $F' = 3$ by the cooling laser only and the last factor indicates the rate at which the atoms come to the F = 2 level by the spontaneous decay.

Similarly, the rate at which the repumper laser transfers atoms from F = 2 to F = 3 through $F' = 3$ is

$$\eta_{23} = \Gamma_{3'2} \frac{\frac{I_r}{I_{s23'}}}{[1 + 2(I_r/I_{s23'}) + 4(\Delta_r/\Gamma_{3'2})^2]} \frac{\Gamma_{3'3}}{(\Gamma_{3'3} + \Gamma_{3'2})} \tag{5.6}$$

Where $\Delta_r = \delta_r - \mathbf{k} \cdot \mathbf{v}$, I_r is the intensity of the repumper beam and other symbols have meanings as given earlier. Let us assume that there are N atoms with velocity v. Of these, at a time t, N_3 are taken to be in the level F = 3 and $N - N_3$ in level F = 2, neglecting any small number that may be in the upper levels $F' = 3$ and 4. N_3 should satisfy the rate equation -

$$\frac{dN_3}{dt} = -\eta_{32} N_3 + \eta_{23}(N - N_3) \tag{5.7}$$

$$\Rightarrow \frac{dN_3}{dt} + (\eta_{32} + \eta_{23}) N_3 = \eta_{23} N \tag{5.8}$$

The solution to the above equation is a sum of (1) the solution of the auxiliary equation and (2) the particular integral. The auxiliary equation

$$\frac{dN_3}{dt} + (\eta_{32} + \eta_{23})N_3 = 0 \tag{5.9}$$

has the solution

$$N_3(t) = N_0 \exp^{-(\eta_{32}+\eta_{23})t} \tag{5.10}$$

where N_0 is a constant to be determined. The particular integral for the equation 5.8 is

$$N_3(t) = \frac{\eta_{23}N}{D + (\eta_{32} + \eta_{23})} \tag{5.11}$$

$$\approx \frac{\eta_{23}N}{\eta_{32} + \eta_{23}} \tag{5.12}$$

where D= $\frac{d}{dt}$. The complete solution to the equation (5.8) is

$$N_3(t) = \left[N_0 \exp^{-(\eta_{23}+\eta_{32})t} + \frac{\eta_{23}}{\eta_{23} + \eta_{32}}N\right] \tag{5.13}$$

The initial condition is at t = 0, $N_3(0) = N_{30}$. Therefore, from equation (5.13) we have

$$N_0 = \left[N_{30} - \frac{\eta_{23}}{\eta_{23} + \eta_{32}}N\right] \tag{5.14}$$

Substituting this value in the equation 5.13, we get

$$N_3(t) = \left[N_{30} - N\frac{\eta 23}{\eta_{23} + \eta_{32}}\right] \exp^{-(\eta_{23}+\eta_{32})t} + \frac{\eta_{23}}{\eta_{23} + \eta_{32}}N \tag{5.15}$$

We see that the first term decays at a rate $\tau = \frac{1}{\eta_{32}+\eta_{23}}$ and the steady state value of the population in level F=3 is given by the second term.

For numerical calculation we take the following values for the parameters pertinent to our experimental situation: $(I_c/I_{s34'}) = 0.8$, $(I_c/I_{s33'}) = 0.6573$, $(I_r/I_{s23'}) = 0.01$, $\Gamma_{3'3} = 2\pi \cdot 2.59 \cdot 10^6$, $\Gamma_{3'2} = 2\pi \cdot 2.07 \cdot 10^6$, and one value of the detuning $\delta_c = -2\pi \cdot 60 \cdot 10^6$ Hz. An atom with speed $v_c = |\delta_c|/k$ (k is the wave vector of the cooling beam) moving parallel to the beam will see that the cooling laser is on resonance, and therefore, $\delta_{4'3} = 0$. $\delta_{3'3} = -2\pi \cdot 121 \cdot 10^6$ MHz. For these values of the detunings $\eta_{32} = 552$. If we choose $\delta_r = -2\pi \cdot 120 \cdot 10^6$, $\eta_{23} = 21.4$. Therefore,

$$\tau_{decay} = 1/576 = 1740\ \mu s.$$

From the above example we see that at double resonance $\delta_r = \delta_c$, then $\Delta_{33'} = 2\pi \cdot 121 \cdot 10^6$ MHz, $\delta_{23'} = 0$. Then $\eta_{32} = 552$, $\eta_{23} = 7.08 * 10^4$. So

$$\tau_{decay} = 1/(7.08 * 10^4) = 14\ \mu s.$$

much less than the time taken by the atom to cross the molasses region. The steady state distribution will be reached very quickly. This stationary number of atoms in level 3 will be in the cooling cycle for the residence period and the atoms will be slowed down.

Having calculated the number of atoms in level $F = 3$ for different detunings of the repumper laser δ_r around a fixed detuning δ_c of the cooling laser, we next calculate the expected fluorescence. The fluorescence from atoms with a given entrance velocity v is proportional to the fraction $\frac{\eta_{23}}{\eta_{23}+\eta_{32}}$ multiplied by the spontaneous transition probability from $F' = 4'$ to $F = 3$ taking into account the Doppler shift caused by the motion of the atom. This product is integrated for all velocities to get the fluorescence intensity for a given value of δ_c and δ_r

At double resonance, $\eta_{23} >> \eta_{32}$ (because of the $\Delta_{3'3}$ in the denominator of η_{32}), N_3 rises rapidly from N_{30} to nearly N with a rise-time of a few tens of microseconds, and the fluorescence is maximised. Away from double resonance, the fluorescence is much smaller, as has been estimated using equation (5.15) and as is shown in figure 5.8. The fluorescence is maximum when $|\delta_r| = \delta_c$ with a FWHM of about 40 MHz that is governed by the velocity range of the atoms which contribute to the fluorescence effectively.

Our laser has a narrow line width of < 1 MHz. Energy levels also have a natural linewidth. In addition the levels are power broadened by 2.4 MHz in our case. All these effects contribute to atoms with a range of velocities around v_c to satisfy the double resonance condition and cause the width of the fluorescence peak. Collisional broadening is negligible at the low pressure in the vacuum chamber. This simple rate analysis also gives a reasonable explanation for the narrow fluorescent peaks in the fluorescence despite the presence of a thermal

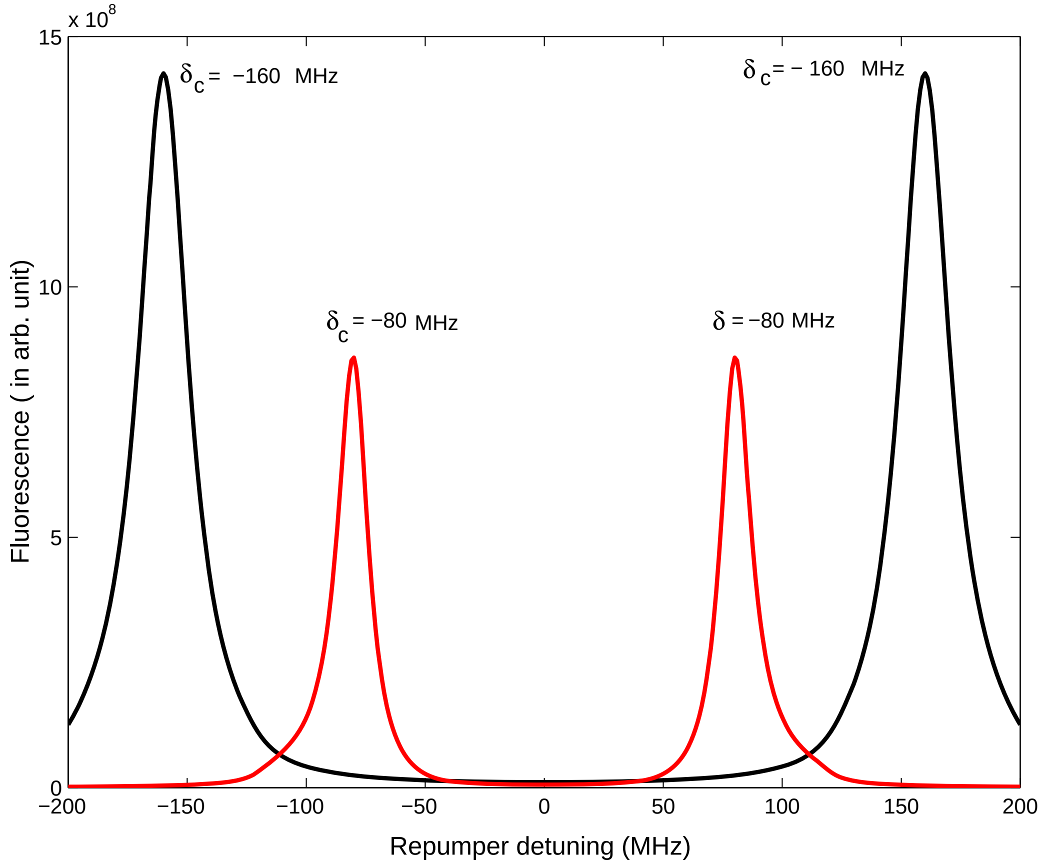

Figure 5.8: Fluorescence estimated using equation (14) for $\delta_c = -160$ MHz (black) and $\delta_c = 80$ MHz (red).

velocity distribution.

The fluorescence is due to the spontaneous emissions of the photons when the atomic transitions take place from $F' = 4' -> F = 3$, $F' = 3' -> F = 3$, $F' = 3' -> F = 2$. Out of the three transitions $F' = 4' -> F = 3$ has the maximum contribution to the total fluorescence. The intensity at the fluorescence depends upon the number of atoms participating in the transition. The $F' = 4' -> F = 3$ transition is a closed transition. Therefore, the number of atoms participating depends upon the population in the $F = 3$ level. The population can also be high due to two reasons and the fluorescence peak can be very large. This is discussed below:

The excess population in level $F = 3$ builds up for two different reasons.

1. Redistribution of the atoms between $F = 2$ and $F = 3$ levels by the repumper laser beams at the double resonance:

   when the atoms enter the molasses region they have a 50% probability of being in state F = 2 or F = 3. When the double resonance condition is far from being satisfied the repumper efficiency in transferring atoms from F = 2 to F = 3 is very poor. This results in a depletion of atoms from level F = 3. On the otherhand at double resonance ($\delta_r = \pm \delta_c$) the repumper becomes very efficient in transferring atoms from level F = 2 to F = 3. In a few tens of microseconds the population in level F = 3 grows to nearly 100%. This is shown in figure 5.9. This increase in the number of atoms in F = 3 gives rise to a peak in the fluorescence.

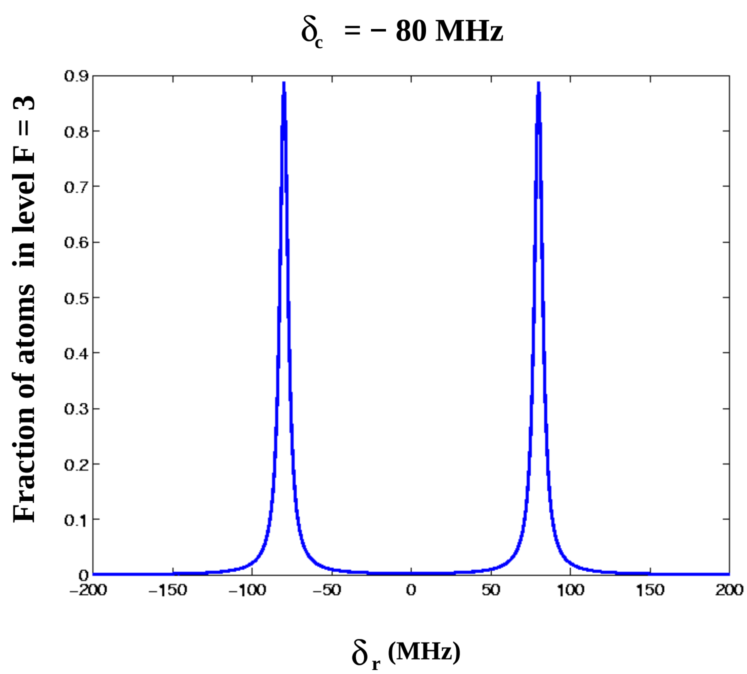

Figure 5.9: Fraction of atoms in F = 3 as a function of repumper detuning δ_r, for a cooling laser detuning δ_c = -80 MHz.

2. The excess residence time of the atoms in the optical molasses region:

the atoms feel a damping force in the optical molasses due to the cooling laser and the velocity gets reduced. Therefore, the atom resides in the molasses region for a longer time compared to the situation when the atoms are not slowed. Slowing of the atoms by cooling beams with a given detuning δ_c is most effective for atoms with speed close to the value $v_c = |\delta_c|/k$. The excess residence time for this class of atom increases the number density in the molasses and causes a peak in the fluorescence. This effect occurs only when the cooling beam is red detuned. However this effect is not as important as the redistribution of the population of atoms (figure 5.10)

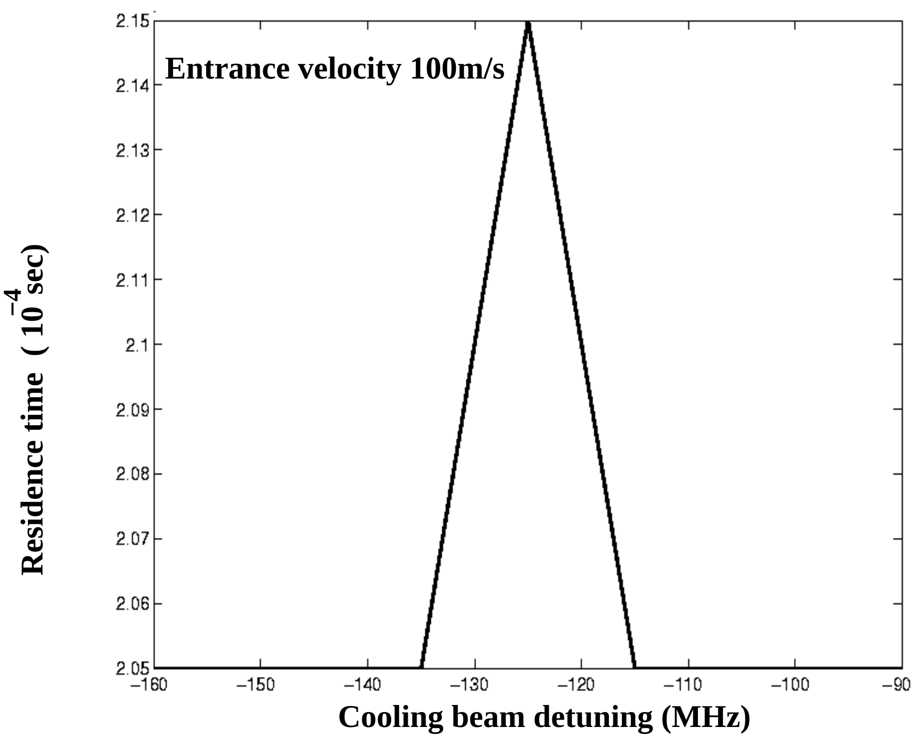

Figure 5.10: Residence time in molasses for different cooling beam detunings. T_{nomol} = 200 μsec, the curve peaks at δ_c = -125 MHz, Doppler shift for entrance velocity is 128 MHz. The maximum increase in the residence time is about 7% only.

In a similar experimental condition we have also studied the fluorescence signal from a cold atom cloud in a Magneto-Optical-Trap (MOT). Inside a MOT, Zeeman splitting of the atomic energy levels take place. Therefore, the narrow dips in the fluorescence signal for small detuning ($\approx$ 10 MHz) of the cooling laser are not visible.

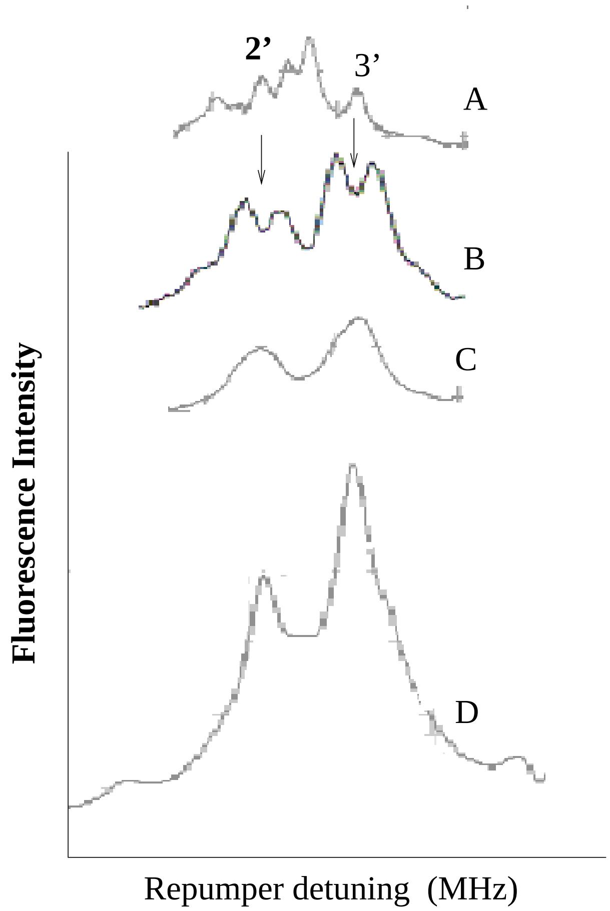

Figure 5.11: Oscilloscope traces of (A) saturated absorption spectrum of repumper; fluorescence traces from (B) 3-D optical molasses, (C) MOT and (D) 1-D optical molasses in Rb vapour cell. Cooling laser detuning is δ_c = -10 MHz for all the traces.

For example, in trace C in figure 5.11, which is the fluorescence from the MOT, broad peaks are seen due to double resonance. The dips shown by arrows in trace B, which is for fluorescence from 3D optical molasses, are not seen. This is understandable as, in a MOT, the presence of spatially varying magnetic field causes a broadening of the peak and narrow features are smeared out.

We have also repeated these experiments in a 1-D optical molasses formed in a vapour cell. The fluorescence trace shown as D in figure 5.11 for the same detuning δ_c of approxi-

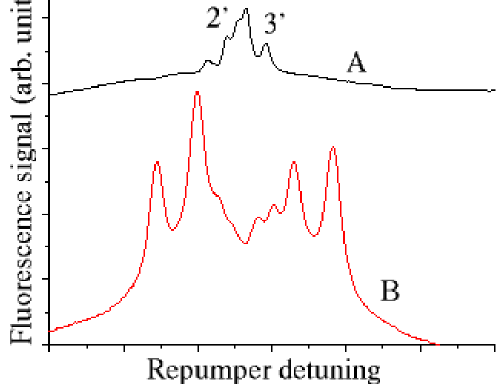

Figure 5.12: Oscilloscope traces (A) saturation absorption signal for repumper ; (B) fluorescence from molasses for δ_c = - 110 MHz (Red).

mately -10 MHz. Again while we see the double resonance peaks, the narrow dips in trace B are not visible. As the pressure inside the vapour cell is higher than that in the UHV chamber, collisional broadening will be more (as the buffer gases are also present in the vapour cell). Therefore the fluorescence peaks are not resolved for low detuning of the cooling beam. But as the detuning of the cooling beam is increased the results are similar to those obtained from 3D optical molasses with very low presure.

5.5 Additional peaks at larger detuning

Thus far, we have explained the narrow fluorescence peaks using "double - resonance" - a phenomenon in which atoms within a small range are selected out, such that both the lasers appear on resonance with their respective transitions. Thus, for a fixed value of δ_c we expect double resonance fluorescence peaks at 4 different values of δ_r, namely δ_r = + δ_c, - δ_c, + δ_c - 63, - δ_c - 63, corresponding to the two repumping transitions.

In a further set of experiments, the cooling laser was locked at larger detunings, and the repumper laser ramped over larger ranges. As against the four prominent peaks of the earlier experiments, numerous more peaks appeared as may be seen from figures 5.12 to 5.17. In these figures trace A represents the saturated absorption signal for repumper beam and trace B the fluorescence signal. We explain the prominent peaks using the double-resonance model.

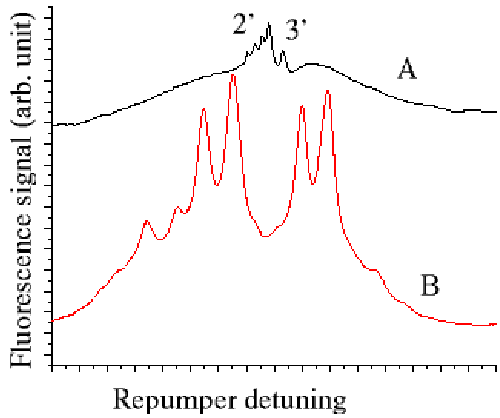

Figure 5.13: Oscilloscope traces (A) saturation absorption signal for repumper ; (B) fluorescence from molasses for δ_c = + 110 MHz (blue).

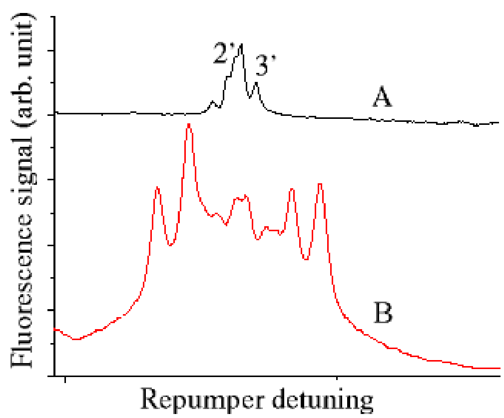

Figure 5.14: Oscilloscope traces (A) saturation absorption signal for repumper ; (B) fluorescence from molasses for δ_c = -140 MHz (Red).

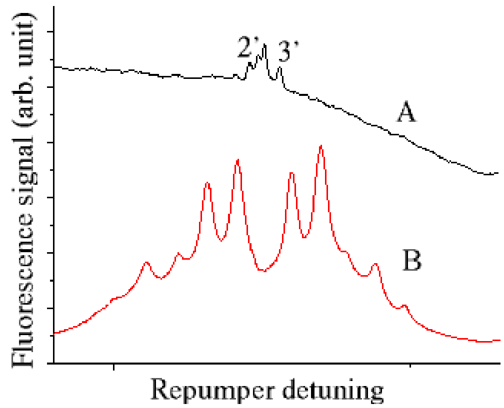

Figure 5.15: Oscilloscope traces (A) saturation absorption signal for repumper ; (B) fluorescence from molasses for δ_c = + 140 MHz (blue).

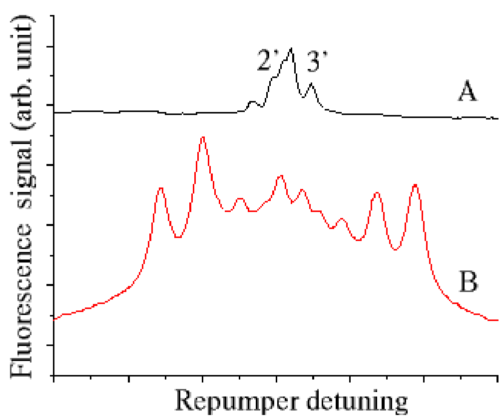

Figure 5.16: Oscilloscope traces (A) saturation absorption signal for repumper ; (B) fluorescence from molasses for δ_c = - 170 MHz (Red).

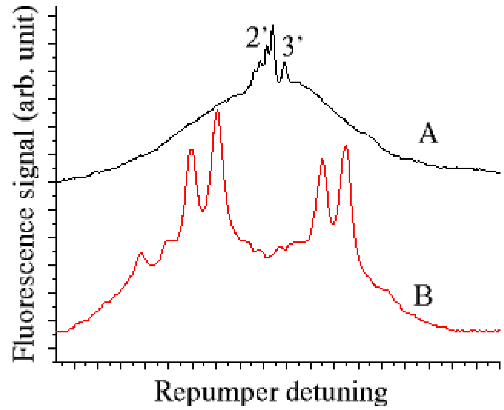

Figure 5.17: Oscilloscope traces (A) saturation absorption signal for repumper ; (B) fluorescence from molasses for δ_c = + 170 MHz (Blue).

It is to be noted that when the cooling laser detuning δ_c is defined with respect to F = 3 to F′ = 4 transition, it has a detuning δ_c + 121 and δ_c + 184 with respect to F = 3 to F′ = 3 and F = 3 to F′ = 2 transitions respectively. This laser can then excite atoms with velocity v = $|\delta_c|/k$ to the cooling transition F = 3 to F′ = 4. The same laser can also excite atoms with velocity v' from F = 3 to F′ = 3 transition and velocity v'' to F = 3 to F′ = 2, where v' = $|\delta_c + 121|$/ k and v'' = $|\delta_c + 184|$/ k .

Thus, double resonance can occur for various pairs of transitions ($2->3'$, $3->4'$); ($2->2'$, $3->4'$), ($2->3'$, $3->3'$);($2->2'$, $3->3'$), ($2->3'$, $3->2'$); ($2->2'$, $3->2'$). These should give fluorescence peaks at δ_r = + δ_c, - δ_c, + δ_c - 63, - δ_c - 63, δ_c + 121, - δ_c - 121, + δ_c + 58, - δ_c - 184, δ_c + 184, - δ_c -184, + δ_c + 121, - δ_c - 247. The plot δ_c versus δ_r must give rise to twelve lines out of which two pairs of lines fall on top of each other. Therefore there are ten independent straight lines with slopes ±1, which intersect at different points labelled A,B, C,D,E and F. This is illustrated in figure 5.18. The separation in frequency between the pair of points A, B (or C, D or E, F) 63 MHz.

For a given δ_c one can draw a vertical line through that value. This line will cut the ten lines at ten values of δ_r which will be well resolved when the detuning is large.

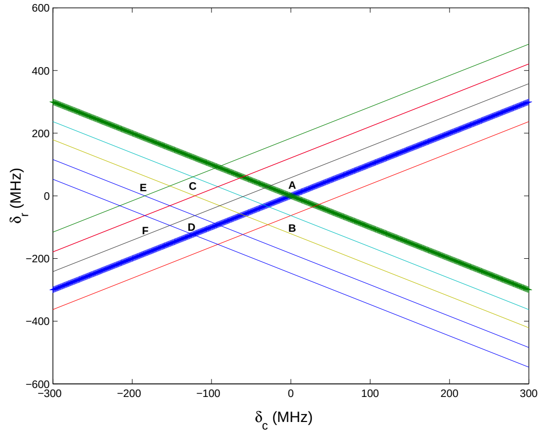

Figure 5.18: Shift of the positions of the fluorescence peaks due to the variation of the cooling laser detuning

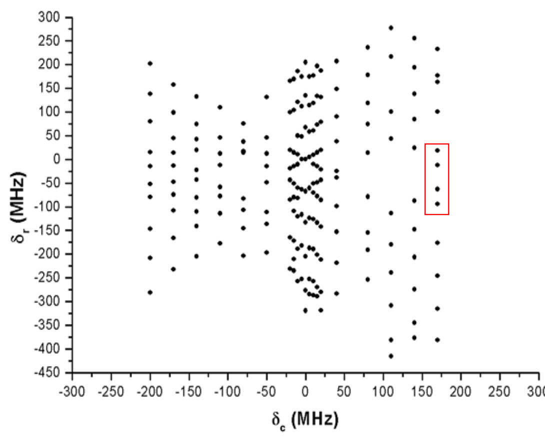

Figure 5.19: Positions of the peaks obtained from experiments

δ_c	-170		-140		-110		+110		+140		+170	
Pk. no.	expt	calc	expt	calc	expt	calc	expt	calc	expt	calc	expt	calc
1	158	170	133	140	109	110	277	294	255	261	277	291
2	99	107	74	77	46	47	217	231	194	198	233	228
3	45	49	43	44	12	11	101	110	139	140	164	170
4	14	14	21	19	-12	-11	44	47	85	77	101	107
5	-14	-14	-22	-19	-58	-52	-113	-110	-	-	-176	-170
6	-47	-49	-43	-44	-78	-74	-180	-173	-148	-140	-245	-233
7	-108	-112	-81	-82	-114	-110	-239	-231	-207	-202	-241	-245
8	-167	-170	-142	-140	-177	-173	-308	-294	-275	261	-315	-291
9	-232	-233	-205	-203	-	-	-	-	-	-	-381	-354

Table 5.1: Comparison of positions (δ_r) of the experimental and calculated peaks for cooling beam detunings shown in figures 5.12 to 5.17. The numbers given in the table are in MHz.

These ten values correspond to the peaks observed in the experiment. The experimental points are plotted in figure 5.19. Table 5.1 compares the positions of the experimental peaks (δ_r values) shown in figures 5.12 to 5.17 with the calculated values. Considering that the fluorescence peak widths are of the order of 30MHz, agreement between the experimental and calculated values is good. This shows the explanation offered is the correct one.

We also observe a few additional peaks which do not fall on the lines in figure 5.18. The four points in the box in figure 5.19 are such example. We have not established the full explanation for these points as yet. From the discussion given in Chapter 6, it appears that these are AT levels of the F′ = 2 and 3 levels. However, further analysis is needed to confirm this.

5.6 Unequal peak heights

We find the daughter peaks in the fluorescence signal are unequal in heights (see figure 5.3 and 5.4). The reason can be due to the unequal intensities in the counter-propagating beams. The retro-reflected beam always has a lower intensity than the forward beam especially as the windows of the MOT chamber are not anti-reflection coated. This may be a reason for the unequal heights of the peaks. Same feature was found in the fluorescence signal from the 1D optical molasses in the Rb vapour cell. In this case the height difference is more probably due to the larger amount of Rb present in the cell.

5.7 Conclusions

Fluorescence [1] from an optical molasses in ^{85}Rb in the presence of a pump (cooling) and probe (repumper) laser shows splitting of peaks, with the separation increasing linearly with the detuning of the pump. A simple model explains both the peak positions and their narrow linewidth as arising from velocity selection due to the requirement of the simultaneous Doppler resonance. It also provides a means of selecting out atoms of a narrow velocity range from a hot gas.

[1] I thank Dr. C. S. Unnikrishnan, TIFR, Mumbai, for lending me the femtoWatt detector.

Bibliography

[1] C. Cohen-Tannoudji. and S. Reynaud, Journal of Physics B **10**, 365(1977).

[2] S. H. Autler and C. H. Townes, Physical Review **100**, 703(1955).

[3] G. S. Agarwal, Physical Review A **54**, 3734(1996).

[4] G. Vemury, G. S. Agarwal and B. D. Nageswara Rao, Physical Review A **53**, 2842(1996).

[5] Laser Cooling and Trapping, H.J. Metcalf and P. van der Straten (Springer-Verlag New York, Inc. (1999)).